

# Preparation and Characterization of Isotropic Polyurethane Magnetorheological Elastomer Through *In Situ* Polymerization

Jinkui Wu,<sup>1</sup> Xinglong Gong,<sup>2</sup> Lin Chen,<sup>2</sup> Hesheng Xia,<sup>1</sup> Zaiguo Hu<sup>3</sup>

<sup>1</sup>State Key Laboratory of Polymer Materials Engineering, Polymer Research Institute of Sichuan University, Chengdu 610065, China

<sup>2</sup>CAS Key Laboratory of Mechanical Behavior and Design of Materials, Department of Modern Mechanics, University of Science and Technology of China, Hefei 230027, China

<sup>3</sup>Physical Department, Sichuan University, Chengdu 610065, China

Received 6 December 2008; accepted 5 April 2009

DOI 10.1002/app.30563

Published online 15 June 2009 in Wiley InterScience (www.interscience.wiley.com).

**ABSTRACT:** The highly filled isotropic polyurethane (PU) elastomer with a magnetorheological (MR) effect was prepared through an *in situ* polycondensation method. The carbonyl iron particles were treated by coupling agents and then the dispersions of polyol/carbonyl iron particles was prepared by a ball milling process. The dispersion problem of magnetizable particles at a high content in PU matrix was tried to overcome by the combination of surface modification, ball milling, and *in situ* polymerization. The microstructure and properties of the composite were examined in detail. With increasing the content of carbonyl iron particles, the degree of phase separation of PU increased and the glass transition temperature ( $T_g$ ) of PU soft segment decreased. Highly filled carbonyl iron particles led to the decrease in the thermal stability of PU matrix, especially in the heating air atmosphere. The MR effect appeared when

the content of carbonyl iron particles was higher than 50 wt %, and became relatively pronounced at a 70 wt % of carbonyl iron content. The mechanical properties of PU MR elastomers were deteriorated significantly at a high content of carbonyl iron. Surface modification of carbonyl iron particles can improve the mechanical properties to some extent; however, it was also found that surface modification led to a decrease in the MR effect because of the improved interfacial adhesion. The MR test showed that the maximum absolute MR effect and relative MR effect of PU composite were  $\sim 0.31$  MPa and  $\sim 8.1\%$  at 1 Hz and 400 mT with 70 wt % of carbonyl iron, respectively. © 2009 Wiley Periodicals, Inc. *J Appl Polym Sci* 114: 901–910, 2009

**Key words:** polyurethane; magnetorheological elastomer; *in situ* polymerization; ball milling dispersion

## INTRODUCTION

Magnetorheological (MR) materials belong to a family of so-called smart material whose rheological properties can be controlled rapidly and reversibly by the application of external magnetic field. MR fluids are the most famous MR material whose research history could be traced back to as early as 1948.<sup>1</sup> The MR fluid comprised magnetizable particles and a nonmagnetic carrier medium. The rheological properties of MR fluid can be controlled continuously, rapidly, and reversibly by external magnetic field, which makes MR fluid commercially available for a variety of applications, such as vehicle seat

vibration control<sup>2</sup> and primary automotive suspensions.<sup>3</sup> However, the MR fluid has some shortcomings: (i) the particles tend to settle out in the suspension over a period because of the density mismatch between the particles and the carrier medium and (ii) the appropriate seals are needed to prevent any leakage of the MR fluid during the service.<sup>4</sup>

To solve those problems, the MR elastomers in a solid state were developed firstly by Shiga et al.<sup>5</sup> Since then, it has attracted the scientific and practical interests.<sup>6–18</sup> MR elastomers are similar to MR fluids in structure except that an elastic matrix replaced the fluid carrier. The obvious advantage of using elastomers is that the particles are not able to settle with time and that there is no need to use containers to keep the MR material in its place. According to the orientation of the magnetizable particles, MR elastomers can be divided into isotropic and anisotropic MR elastomers. The matrix for MR includes soft silicon rubber,<sup>5–9</sup> natural rubber,<sup>10,11</sup> nitrile rubber,<sup>12,13</sup> isobutylene and isoprene rubber,<sup>14</sup> and polyurethane.<sup>15–18</sup> The conventional procedure to prepare MR elastomers was directly mixing the

Correspondence to: H. Xia (xiahs@scu.edu.cn).

Contract grant sponsor: National Science Foundation of China; contract grant number: 50673060.

Contract grant sponsor: National Basic Research Program of China (973 Program); contract grant number: 2007CB714701.

rubber with the magnetizable particles and then conducting the vulcanization the same as the manufacturing process of carbon black-filled rubber. One problem is the dispersion of magnetizable particles at a high content up to 70% in the rubber matrix, and another problem is the aging of rubber under the influence of carbonyl iron.

Recently, polyurethane-based MR elastomers have attracted much attention.<sup>15–18</sup> Typical PU elastomers are (AB)<sub>n</sub>-type multiblock copolymers comprised alternating soft polyether or polyester segments and hard segments based on isocyanate and chain extender. The properties of PU elastomers such as tensile strength, stiffness, friction coefficient, and chemical resistance can be easily adjusted by changing polyol type, hard segments content, etc.<sup>19</sup> PU elastomers have the potential for MR application in practice because of its versatility.

In this article, we prepared highly filled isotropic polyurethane elastomers with magnetorheological effect through *in situ* polymerization method. The dispersion problem of magnetizable particles at a high content in PU matrix was tried to overcome by our procedure. PU elastomer, with a hard segment content of 26% using the flexible polytetramethylene ether glycol (PTMEG) as the soft segments, was used as the matrix for MR elastomer. The interaction between the carbonyl iron and PU matrix were investigated. The effect of carbonyl iron on the microstructure, thermal, mechanical, and MR properties were studied in detail.

## EXPERIMENTAL

### Materials

4, 4'-methylene-di (phenylene isocyanate) (MDI), supplied by Yantai Wanhua Polyurethanes Co., Ltd., China, was used as received without further purification. Polytetramethylene ether glycol (PTMEG,  $M_n = 1000$ , provided by Mitsubishi Chemical Holdings Corporation) was dehydrated in a vacuum oven at 120°C for 1 h before use. 1, 4-butanediol (BDO), provided by Chengdu Kelong Chemical Factory, China, was redistilled to remove water before use. Polyoxypropylene glycol (PPG,  $M_n = 3000$ ) was obtained from the Third Petrochemical Factory, Tianjin Petrochemical Inc., China. The spherical carbonyl iron particles (FTF-1), with a size range of 3–5 μm, was purchased from Hebao Nanomaterial Co., Ltd, China. The catalyst Dabco-33LV was obtained from Air Products and Chemicals. The antifoam agent BYK-535 was provided by Sino Composite Co., Ltd., China. 3-aminopropyltriethoxysilane (KH-550) and 3-glycidoxypropyltrimethoxysilane (KH-560) were purchased from Chenguang Chemical Co., Ltd., China. Aminoethylamino-propyltrimethoxysilane (Z-

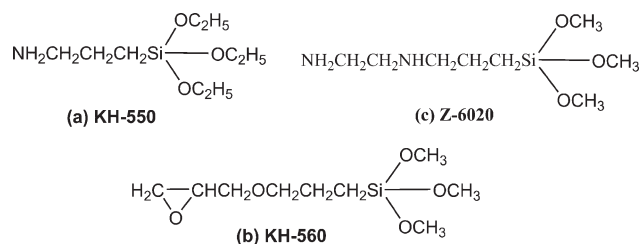


**Figure 1** The chemical structure of silane coupling agents: (a) KH-550, (b) KH-560, and (c) Z-6020.

6020) was kindly provided by Dow Corning. The chemical structure of KH-550, KH-560, and Z-6020 were shown in Figure 1.

### Surface treatment of carbonyl iron

Silane coupling agent (2.5 g), 22.5 g of distilled water, and 225 g of ethanol were added into a three-necked flask equipped with a condenser and a mechanical stirrer, the pH value of the mixed solution was adjusted with acetic acid to ~ 4.0. The mixed solution was stirred for 5 min to assure the hydrolyzation of the silane coupling agent. Then 250 g of carbonyl iron particles was added. The mixture was stirred for 4 h at 80°C, and filtered and washed with ethanol. Finally, the surface-treated carbonyl iron was dried in vacuum for 4 h at 110°C.

### Preparation of PU-carbonyl iron (PU-Fe) composites

1. Preparation of the polyol-carbonyl iron dispersion: Typically, 70.00 g of melted PTMEG and 141.89 g of carbonyl iron were added to the jar, and mixed by ball milling for 1 h to obtain polyol-carbonyl iron dispersion.
2. Preparation of PU-Fe composites: The PU-Fe composites were prepared by a one-step *in situ* polycondensation method in which diisocyanate, polyol, and chain extender were reacted together. The hard segment content of PU matrix was 26%. The -NCO/OH ratio was kept at 1.1 : 1 for each sample. Typically, 181.62 g of polyol-carbonyl iron dispersion was blended with 19.96 g of MDI, 1.12 g of BDO, 0.03 g of Dabco-33LV, and 0.05 g of BYK-535 at room temperature for ~ 2 min, and then the mixture was vacuum degassed for 3–5 min to remove the bubbles. At last, the viscous prepolymer was poured into an O-ring metal mold and cured at 120°C for 24 h, then was cooled to room temperature and kept for two weeks to obtain the PU-Fe composite elastomer at a 60 wt % of carbonyl iron content. As a contrast, PU-Fe composite with different content of carbonyl iron were prepared with the same procedure.

## Characterization

### Tensile test

The tensile test was performed on the dumbbell-shaped specimens with an Instron 5567 universal testing instrument at room temperature. The specimens were stretched until break at a crosshead rate of 500 mm/min. The stress-strain curves were recorded. The tensile strength, elongation, and stress at 100, 200, and 300% strain were the average values of five specimens.

### Fourier transform infrared spectra

Fourier transform infrared spectra (FT-IR) spectra measurements were performed on a Nicolet 560 FT-IR spectrometer by a ATR mode, the spectra were collected from 4000 to 400  $\text{cm}^{-1}$ , with a 4  $\text{cm}^{-1}$  resolution over 32 scans.

### Scanning electron microscope

A JEOL JSM-5900LV scanning electron microscope (SEM) instrument was used to observe the morphology of the fractured surfaces and the dispersion of carbonyl iron particles in the matrix using an acceleration voltage of 20 kV. The samples were cryogenically fractured in liquid nitrogen. The fractured surfaces of the specimens were sputter coated with a thin gold layer before SEM observation.

### Thermal conductivity

The thermal conductivity of PU and PU-Fe composite were measured on a Hot Disk 2500 thermal constant analyzer, which was based on a transient technique. The measurements were performed with specimens (50 mm  $\times$  50 mm  $\times$  3 mm) by putting the sensor (3 mm in diameter) between two similar slabs of material. The sensor supplied a heat pulse of 0.03 W for 20 s to the sample at room temperature, and the associated change in temperature was recorded. The thermal conductivity of the samples were obtained.

### Differential scanning calorimeter (DSC)

DSC was used to investigate the thermal properties of PU-Fe composite on a NETZSH 204 DSC instrument in nitrogen atmosphere. About 5–10 mg samples were first cooled to  $-100^\circ\text{C}$  with liquid nitrogen, and then heated to  $150^\circ\text{C}$  at a heating rate of  $10^\circ\text{C min}^{-1}$ .

### Thermogravimetric analysis (TGA)

TGA was performed on a TGA Q600 equipment (TA Instrument) in the nitrogen and air atmosphere,

respectively, to characterize the thermal stability of samples at different carbonyl iron contents. The samples were heated from  $30^\circ\text{C}$  to  $700^\circ\text{C}$  at a heating rate of  $10^\circ\text{C min}^{-1}$ .

### The magnetorheological effect analysis

Test of MR effect were conducted on a modified dynamic mechanical analyzer (DMA) (Triton Technology Ltd., UK, model Triton 2000B) at room temperature.<sup>20</sup> A shaft connects the sample and the motor in DMA. The motor drive the shaft and the sample moves at given amplitude and frequency. The stress in the sample is measured with the sensor, and the strain is taken as the displacement amplitude. The shear modulus is computed from the data of strain and stress. During the test, a testing magnetic field, which can vary from 0 to 400 mT was applied to the sample. The MR effect test samples have dimensions of 10 mm  $\times$  10 mm  $\times$  3 mm. The dynamic strain amplitude was set as 0.3%. The MR effect was test at three different frequencies, i.e., 1, 5, and 10. Hz.

## RESULTS AND DISCUSSION

### The stability of polyol-Fe dispersion

As the curing of the prepolymer is a slow process, the stability of the polyol-carbonyl iron dispersion has a direct influence on the dispersion of carbonyl iron in polyurethane matrix. Because of the incompatibility and big difference in density between carbonyl iron and polyol, it is difficult to attain the good dispersion of carbonyl iron in polyol by direct mixing. In this article, we tried to combine the ball milling method and the surface modification to improve the dispersion stability of polyol-carbonyl iron dispersion. As the PTMEG is a waxy solid at room temperature, we choose the polyoxypropylene glycol (PPG) as dispersion medium to observe the stability of polyol-Fe dispersion for that PPG is a low-viscous liquid at room temperature and has similar structure to PTMEG. Figure 2(a,b) shows the dispersion stability of polyol-carbonyl iron dispersion with 25 wt % of iron mixed by conventional stirring (a) and ball milling (b), respectively. For untreated raw iron particles, it is clear that even after ball milling the dispersion stability of iron particles in polyol is nearly as poor as that after conventional stirring. This should be attributed to the big difference in density of carbonyl iron ( $\sim 7.8 \text{ g/cm}^3$ ) and polyol ( $\sim 1 \text{ g/cm}^3$ ). Hence, it is necessary to modify the carbonyl iron to enhance the interaction between carbonyl iron and polyol. Three kinds of silane coupling agents, i.e., KH-550, KH-560, and Z-6020, were selected to modify the

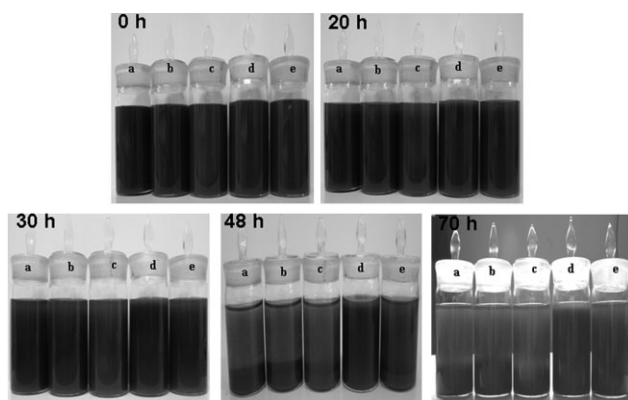


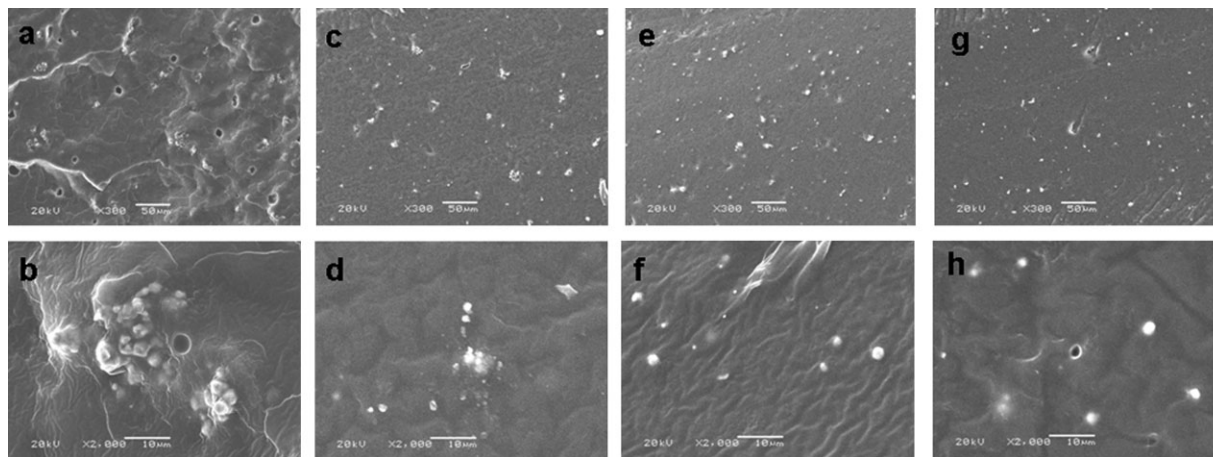
**Figure 2** The dispersion of carbonyl iron particles in polyol obtained by conventional stirring for 3 h (a), and ball milling for 3 h (b–e). (a) and (b) raw carbonyl iron; (c) carbonyl iron treated with KH-550; (d) carbonyl iron treated with KH-560; and (e) carbonyl iron treated with Z-6020.

carbonyl iron. The dispersion effects were shown in Figure 2(c–e). It is clear that the effect of silane coupling agent KH-560 on the stability of carbonyl iron in polyol was better than others. Even after  $\sim 70$  h deposition, the color of the carbonyl iron-polyol dispersion was only slightly changed, and the amount of the settled carbonyl iron was little. This can be attributed to the strong interaction between modified carbonyl iron and polyol. After surface modification, silane coupling agent can be bonded to the surface of carbonyl iron through the condensation reaction of silanol groups and hydroxyl groups on carbonyl iron.<sup>21,22</sup> From the molecule structure of the three silane coupling agents (Fig. 1), we can know that KH-550 and Z-6020 have amino end group, whereas KH-560 have epoxy group and more ether bondings compared with KH-550 and Z-6020. It is the struc-

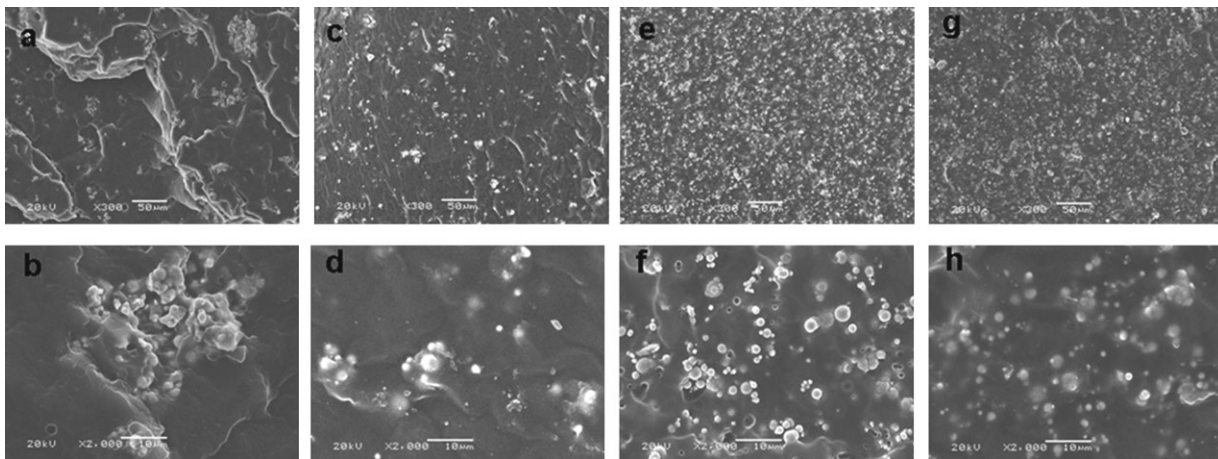
ture similarity of KH-560-treated carbonyl iron and polyol that improved the stability of polyol-Fe dispersion. Consequently, relatively stable carbonyl iron-polyol dispersion can be obtained by the combination of the surface modification with KH-560 and the dispersion effect of ball milling.

### The dispersion of carbonyl iron in PU matrix

A good dispersion of carbonyl iron particles in polyol is the prerequisite for the preparation of well-dispersed PU-Fe composite elastomer. The dispersion of carbonyl iron particles in PU matrix was characterized. SEM photos of the cryogenically fractured surface of PU-Fe composites at 5 wt % of unmodified and modified carbonyl iron particles are shown in Figure 3, respectively. The raw carbonyl iron agglomerated seriously in the matrix [Fig. 3(a,b)]. The dispersion of modified carbonyl iron particles [Fig. 3(c–h)] is greatly improved compared with the unmodified one. The improved dispersion of modified carbonyl iron in PU matrix should be attributed to two points: (i) the relatively stable polyol-carbonyl iron dispersion can reduce the settlement and agglomeration of carbonyl iron in the process of curing and (ii) the amino groups of KH-550 or Z-6020-treated carbonyl iron can react with isocyanate groups of MDI, the epoxy groups of KH-560-treated carbonyl iron can react with isocyanate groups of MDI in the presence of tertiary amine (catalyst Dabco-33LV),<sup>23</sup> this further enhance the interaction between the carbonyl iron and PU molecules. The carbonyl iron particles modified with KH-560 [Fig. 3(g,h)] has the best dispersion effect for the best stability of KH-560 on polyol-Fe dispersion. Figure 4 shows the dispersion of carbonyl iron in PU-Fe composite with a higher content of carbonyl iron.



**Figure 3** SEM of cryogenically fractured surface for PU-Fe composite, the carbonyl iron content was 5 wt %. (a) Raw carbonyl iron, (c) carbonyl iron treated with Z-6020, (e) carbonyl iron treated with KH-550, (g) carbonyl iron treated with KH-560. (b,d,f,h) were the corresponding photos of (a,c,e,g) with higher magnifications.



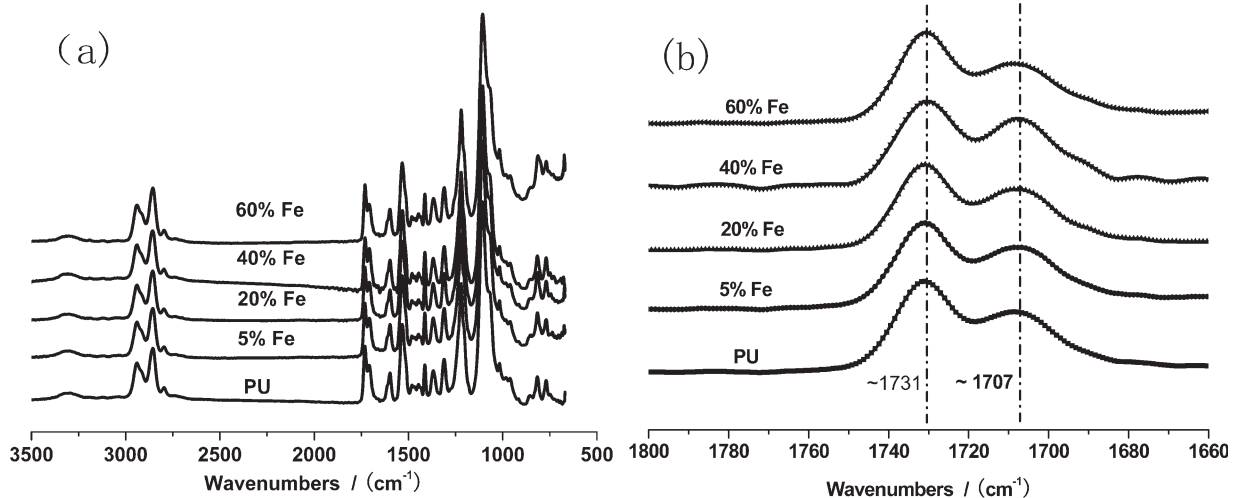
**Figure 4** SEM of cryogenically fractured surface for PU-Fe composite, the carbonyl iron content was 20% in (a–d), and 60% in (e–h). Here, (a,b,e,f) with raw carbonyl iron, (c,d,g,h) with carbonyl iron treated by KH-560. And (b,d,f,h) were the corresponding photographs of (a,c,e,g) with higher magnifications.

Figure 4(a–d) are PU-Fe composite at the 20 wt % of untreated and KH-560 treated carbonyl iron particles, respectively. It can be seen that the dispersion of carbonyl iron in PU matrix improved greatly after the surface modification. Figure 4(e–h) are PU-Fe composite at the 60 wt % of raw carbonyl iron and KH-560 treated carbonyl iron, respectively. A good dispersion at higher content of carbonyl iron in PU matrix was observed as shown in Figure 4 (e,f), even though the carbonyl iron was not modified. The reason maybe is that the higher viscosity for PU-Fe prepolymer at a higher carbonyl iron content prevented the settlement of carbonyl iron during the polycondensation. The interface between the untreated carbonyl iron and PU in the fractured surface is very clear, which indicates that the interaction between the carbonyl iron and PU matrix is weak. After the

modification, the interface between the treated carbonyl iron particles and PU matrix in the fractured surface became more blurry (Fig. 4h), which provided an indirect proof that the compatibility was improved and the interface interaction was stronger.

**FT-IR**

FT-IR spectra of the PU and PU-Fe composite are shown in Figure 5(a), and the attributions of main peaks are shown in Table I. It was found that the positions for the characteristic peaks were identical in both pure PU and PU-Fe composite, which means that the segmented structure of PU was not affected by the presence of carbonyl iron. The characteristic peak of –NCO group at  $\sim 2270\text{ cm}^{-1}$  in IR spectra was not observed, indicating that the reaction of



**Figure 5** FT-IR spectra of PU and PU-Fe composites (a) wavenumbers range:  $500\text{--}3500\text{ cm}^{-1}$  and (b) wavenumbers range:  $1660\text{--}1800\text{ cm}^{-1}$ .

**TABLE I**  
FT-IR Data of PU and PU-Fe Composites

Wavenumbers ( $\text{cm}^{-1}$ )	Attributions
3300–3400	$\nu_{\text{N-H}}$ stretching
2941, 2856	Asymmetric and symmetric $\text{CH}_2$ stretching
1731, 1707	Free and hydrogen bonding $\text{C=O}$ stretching
1597	Breathing vibration of phenyl ring
1533	Amide II $\nu_{\text{C-N}}$ and $\delta_{\text{N-H}}$ vibration
1221	$\nu_{\text{C-O}}$ of ether function from polyether backbone
1107	$\nu_{\text{C-O-C}}$ of polyether backbone

—NCO group was complete. Hydrogen bonding in polyurethane resulted in the phase separation of hard and soft segments. Hydrogen bonding in polyurethanes has been extensively studied using infrared spectroscopy.<sup>24–27</sup> The formation of hydrogen bonding ( $\text{NH}-\text{O}=\text{C}$ ) by  $-\text{C}=\text{O}$  group can be determined by examining the peak position at  $\sim 1707 \text{ cm}^{-1}$  for hydrogen bonded  $-\text{C}=\text{O}$  and at  $\sim 1731 \text{ cm}^{-1}$  for free  $-\text{C}=\text{O}$  [Fig. 5(b)]. By measuring the peak intensity ratio of these two carbonyl groups, it is possible to give an estimate of the degree of hydrogen bonding. The hydrogen bonding index,  $R$ , can be defined as the ratio of absorption peak  $A_{1707}/A_{1731}$ . The peak was fitted by Origin software, and the area of peak at  $1731 \text{ cm}^{-1}$  and  $1707 \text{ cm}^{-1}$  was given, and thus, the hydrogen bonding index  $R$ , the degree of phase separation DPS ( $\text{DPS} = R/(R + 1)$ ), and the degree of phase mixing DPM ( $\text{DPM} = 1 - \text{DPS}$ ) were calculated.<sup>27</sup> The results are shown in Table II. It is evident that with increasing the carbonyl iron content, the hydrogen bonding index and the degree of phase separation increased and thus the degree of phase mixing decreased. Conversely, compared with the blank PU, the interaction between the hard segment and the soft segment decreased as the content of carbonyl iron increased.

### Thermal properties

Figure 6 shows the thermal conductivity of PU and PU-Fe composite with different carbonyl iron content. The thermal conductivity of PU-Fe composite

**TABLE II**  
Hydrogen Bonding Index  $R$ , the Degree of Phase Separation (DPS) and the Degree of Phase Mixing (DPM) for PU and PU-Fe Composites

Fe content (%)	$R (A_{1707}/A_{1731})$	DPS	DPM
0	1.33	0.57	0.43
5	1.39	0.58	0.42
20	1.46	0.59	0.41
40	1.60	0.62	0.38
60	1.61	0.62	0.38

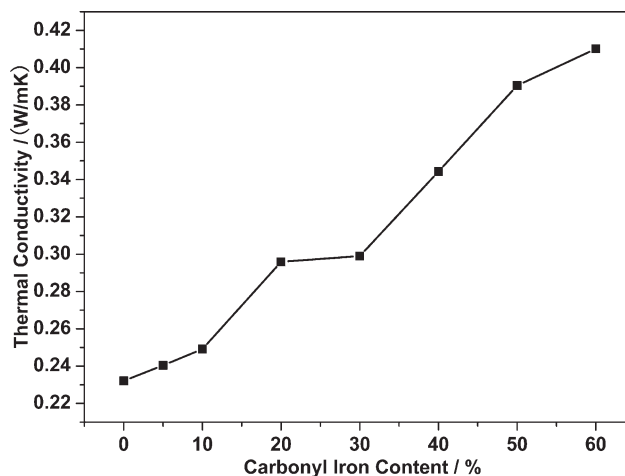


**Figure 6** The thermal conductivity of PU-Fe composite with different carbonyl iron contents.

increased as the carbonyl iron content increased. The thermal conductivity of PU-Fe composite with 60 wt % of carbonyl iron was  $\sim 1.8$  times as that of the blank PU. This is the direct result of incorporation of carbonyl iron with a high thermal conductivity.

The DSC curves for PU and PU-Fe composites are shown in Figure 7, and the results are given in Table III. Glass transition temperatures ( $T_g$ ) of the soft segment chain for blank PU was observed at around  $-41.0^\circ\text{C}$ . With increasing the carbonyl iron content, the  $T_g$  of the soft segment chain decreased. When the carbonyl iron content arrived at 60 wt %, the  $T_g$  of soft segment decreased to  $-49.8^\circ\text{C}$ . The decrease in the  $T_g$  of soft segment should be attributed to the increase in the degree of phase separation, which weakened the interaction between hard and soft segments, and thus make the motion of soft segment easier.

Thermogravimetric analysis (TGA) of PU and PU-Fe composite with different carbonyl iron contents

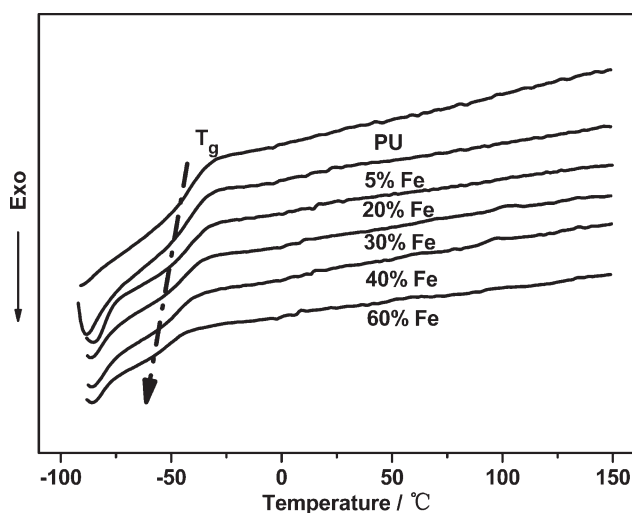


**Figure 7** DSC curves of PU and PU-Fe composite.

**TABLE III**  
The Glass Transition Temperature ( $T_g$ ) of PU and PU-Fe Composite from DSC Curves

Iron content (%)	$T_{\text{onset}}/^{\circ}\text{C}$	$T_{\text{mid}}/^{\circ}\text{C}$	$T_{\text{end}}/^{\circ}\text{C}$
0	-49.2	-41.0	-32.8
5	-49.9	-41.4	-33.0
20	-50.1	-41.6	-33.1
30	-51.6	-43.2	-34.9
40	-53.3	-45.9	-38.5
60	-57.7	-49.8	-41.8

in the nitrogen and air atmosphere are shown in Figure 8, respectively. In general, the thermal degradation of polyurethane occurs in two stages: the initial degradation Stage I is primarily the decomposition of the hard segment, which involves the dissociation of urethane to the original polyol and isocyanate, which then forms a primary amine, alkene, and carbon dioxide. Stage I is influenced by the hard segment content. The consequent Stage II proceeds by the depolycondensation and polyol degradation mechanisms and is affected by the soft segment content.<sup>28</sup> The thermal decomposition temperature of PU and PU-Fe composites in the nitrogen and air atmosphere are shown in Table IV.  $T_{\text{onset}}$  represents the temperature at which the degradation PU matrix starts,  $T_{\text{max1}}$  and  $T_{\text{max2}}$  are the temperature at the maximal thermal degradation rate in Stage I and Stage II, respectively. In the nitrogen atmosphere, the mass of carbonyl iron particles was kept constant during heating and so the mass loss of MR elastomers was entirely due to the thermal degradation of PU. Although in the air atmosphere, the mass of the carbonyl iron particles increased to  $\sim 142\%$  during heating because of the oxidation of carbonyl iron to ferric oxide. From Table IV, it can be seen that in

both atmosphere with the incorporation of carbonyl iron particles,  $T_{\text{onset}}$  and  $T_{\text{max1}}$  decreased. The reason could be that the increase in the thermal conductivity of composites leads to the faster degradation of PU matrix. The  $T_{\text{onset}}$  and  $T_{\text{max1}}$  decreased more in the air atmosphere at the same iron content than that in the nitrogen atmosphere. The possible explanation is that carbonyl iron was oxidized to ferric oxide, and the formed iron ions can catalyze the decomposition and thereby accelerate the oxidation.<sup>29</sup> As  $T_{\text{max2}}$  is affected by the soft segment content, the carbonyl iron has little effect on the  $T_{\text{max2}}$ . In summary, highly filled carbonyl iron will decrease the thermal stability especially in the heating air atmosphere, which is in agreement with the results for natural rubber-based MR elastomers by Lokander et al.<sup>29</sup>

### Mechanical properties

Generally, the content of magnetizable particles in MR elastomers should be higher than 50 wt % to obtain a good MR effect. The deterioration of mechanical properties is a key issue that affects the practical application of the MR elastomers. The mechanical properties of PU and PU-Fe composites with 50, 60, and 70% of raw and treated carbonyl iron are shown in Table V. From Table V, it can be seen that the mechanical properties deteriorated dramatically as the iron content increased from 50 to 70%. The tensile strength of PU-Fe composite decreased from 9.58 to 1.89 MPa, and the elongation at break decreased from 984% to 357%. The deterioration of the mechanical properties of PU-Fe composite should be related to a poor load transfer and the decrease in the degree of phase mixing at a high content of carbonyl iron. From Table V, it can also

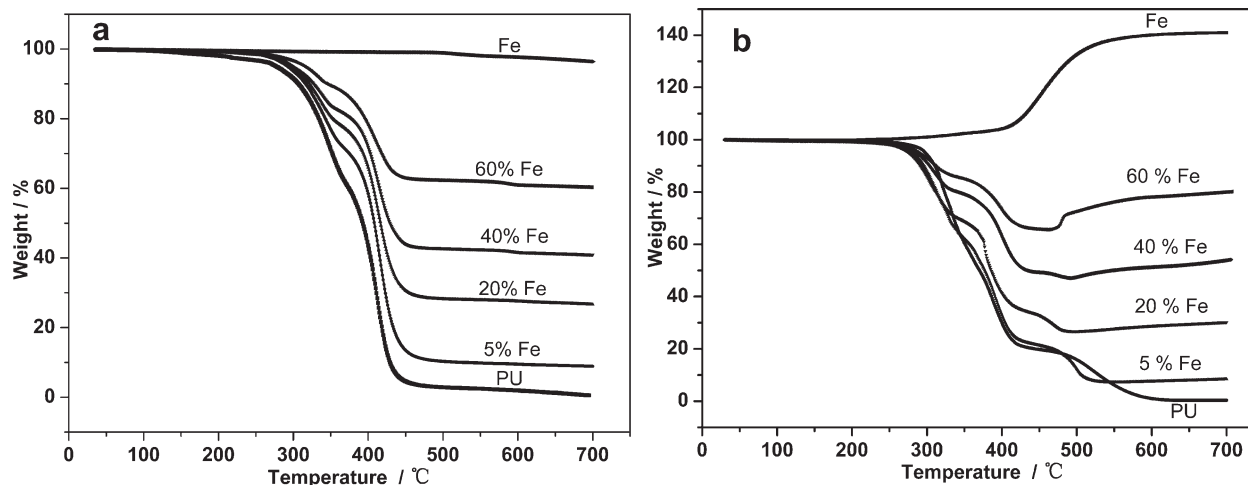


**Figure 8** TGA curves of PU, carbonyl iron, and PU-Fe composite: (a) in the nitrogen atmosphere (b) in the air atmosphere.

**TABLE IV**  
The Thermal Decomposition Temperature of PU and PU-Fe Composite in the Nitrogen and Air Atmosphere from TGA Curves

Iron content (%)	$T_{\text{onset}}/^{\circ}\text{C}$		$T_{\text{max1}}/^{\circ}\text{C}$		$T_{\text{max2}}/^{\circ}\text{C}$	
	Nitrogen	Air	Nitrogen	Air	Nitrogen	Air
0	301.0	300.0	347.8	334.4	411.8	387.0
5	288.8	277.4	344.1	328.0	415.4	390.1
20	285.7	279.0	338.5	312.4	414.2	378.9
40	282.5	276.7	336.9	310.2	413.3	400.1
60	272.6	268.5	335.5	311.0	409.3	399.1

be noted that after the surface modification of iron particles with KH-560, the mechanical properties of PU-Fe composite can be improved to some extent. The tensile strength of PU-Fe composites at 50 and 70% treated carbonyl iron contents increased by  $\sim 26$  and  $\sim 24\%$ , respectively, compared with that for unmodified carbonyl irons. This is because the surface modification can improve the interfacial interaction between the treated iron particles and PU matrix, and lead to an increase in the mechanical properties.

#### MR effect

The isotropic PU magnetorheological elastomer was obtained by *in situ* polycondensation in the absence of magnetic field. When the isotropic PU magnetorheological elastomer are subjected to the magnetic field, carbonyl iron particles tend to align in the direction of the magnetic field for that carbonyl iron can be magnetized easily and soft PU matrix can be deformed. The field-induced magnetic forces between the carbonyl iron particles provide an ability of antideformation, resulting in the change of shear modulus. This should be the origin of the magnetorheological effect.

The variation in the shear modulus of PU magnetorheological elastomer with the contents of untreated and treated carbonyl iron particles under a magnetic field are shown in Figures 9 and 10, respectively. Here,  $G_0$  is the zero-field shear modulus,  $\Delta G$  is the increment of field-induced shear modulus,

i.e., absolute MR effect,  $\Delta G/G_0 \times 100\%$  is relative MR effect. Figures 9(a) and 10(a) showed the zero-field shear modulus at 1, 5, and 10 Hz with different content of untreated and treated carbonyl iron. It can be seen that  $G_0$  increased with the iron content and the test frequency. After surface modification,  $G_0$  was a little higher than that of with raw carbonyl iron at the same iron content and test frequency probably because of the stronger interaction between the particles and PU matrix. The field dependence of shear modulus is shown in Figures 9 and 10(b–d). The MR effect appeared when the content of carbonyl iron particles is higher than 50 wt %, and become relatively pronounced at a 70 wt % of iron particles content. It is very surprised that that the MR effect of PU elastomer containing KH-560-treated carbonyl iron was lower than that of samples containing raw carbonyl iron. The reasons may be that: (i) after the surface treatment, the interaction between the iron and PU matrix is stronger [this was supported from Fig. 4(h)], so the iron particles are difficult to close to each other in the magnetic field compared with the raw carbonyl iron and (ii) the raw carbonyl iron particles tend to aggregate to form larger irregularly shaped particles, thus the interaction of raw carbonyl iron is stronger.<sup>12</sup> It can be noted that the MR effect was higher at a lower test frequency, this is because PU molecular chains have the adequate time to move at a lower frequency, and thus the carbonyl iron particles can move closely easier under a magnetic field, whereas at a higher frequency, the PU molecular chains tend

**TABLE V**  
Mechanical Properties of PU and PU-Fe with Raw and Treated Carbonyl Iron Particles

Iron content (%)	Tensile strength/MPa		Elongation at break/%		Stress at 100% strain/MPa		Stress at 200% strain/MPa		Stress at 300% strain/MPa	
	Raw	Treated	Raw	Treated	Raw	Treated	Raw	Treated	Raw	Treated
0		9.54		466		1.78		2.33		3.26
50	9.58	12.07	984	971	1.86	1.92	2.03	2.18	2.32	2.65
60	6.93	7.63	1129	1152	1.66	1.79	1.80	1.97	2.04	2.24
70	1.89	2.34	327	417	1.92	2.23	2.00	2.30	1.99	2.27

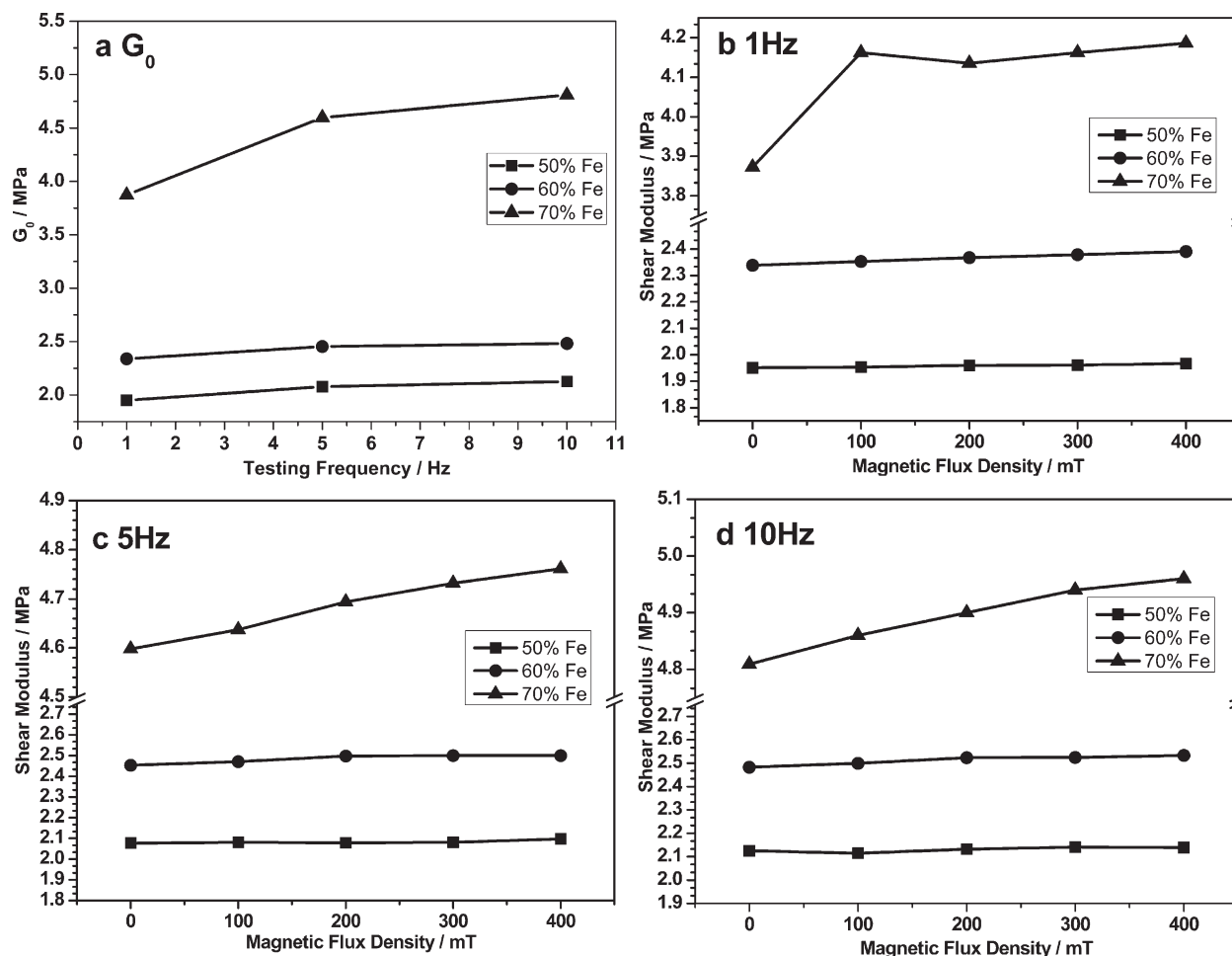


**Figure 9**  $G_0$  and magnetic field-induced shear modulus increment of PU MR elastomer prepared with raw carbonyl iron particles tested at different frequencies: (a)  $G_0$ , (b) 1 Hz, (c) 5 Hz, and (d) 10 Hz.

to be rigid chains for the lack of adequate time to move, so the distance between the iron particles are larger than that at a lower frequency and this results in smaller interaction between carbonyl iron particles, consequently the MR effect is lower. The sample at a 70 wt % of untreated carbonyl iron content has maximum absolute MR effect and relative MR effect, i.e., 0.31 MPa and 8.1%, respectively, at 1 Hz and 400 mT. The absolute MR effect for 70 wt % PU-Fe composite elastomers is a little higher than that for 75 wt % Fe/silicon rubber composites developed by Wang et al.<sup>22</sup> This suggests that PU can be a good matrix for MR elastomer.

## CONCLUSIONS

In this article, the highly filled isotropic polyurethane magnetorheological elastomers were prepared by *in situ* one-step polycondensation process. The influences of carbonyl iron particles contents on the microstructure, thermal, mechanical, and MR properties of PU elastomers were investigated.

1. By using the surface modification of carbonyl iron particles and ball milling, the dispersion of carbonyl iron in PU matrix was improved. The surface modification also enhanced the interaction between the carbonyl iron and PU matrix.
2. With the introduction of carbonyl iron particles, the hydrogen bonding index and the degree of phase separation of PU increased. The  $T_g$  of PU soft segment decreased with increasing the carbonyl iron content. Highly filled carbonyl iron particles will reduce the thermal stability especially in the air atmosphere.
3. At high contents of carbonyl iron particles, the mechanical properties of PU MR elastomers were deteriorated significantly, after surface modification, the mechanical properties can be improved to some extent. PU can be a good matrix for MR elastomer. The maximum relative MR effect of 8.1% was obtained at a 70 wt % of unmodified carbonyl iron content. After the surface modification of carbonyl iron particles with KH-560, the MR effects decreased compared with the unmodified one. It was

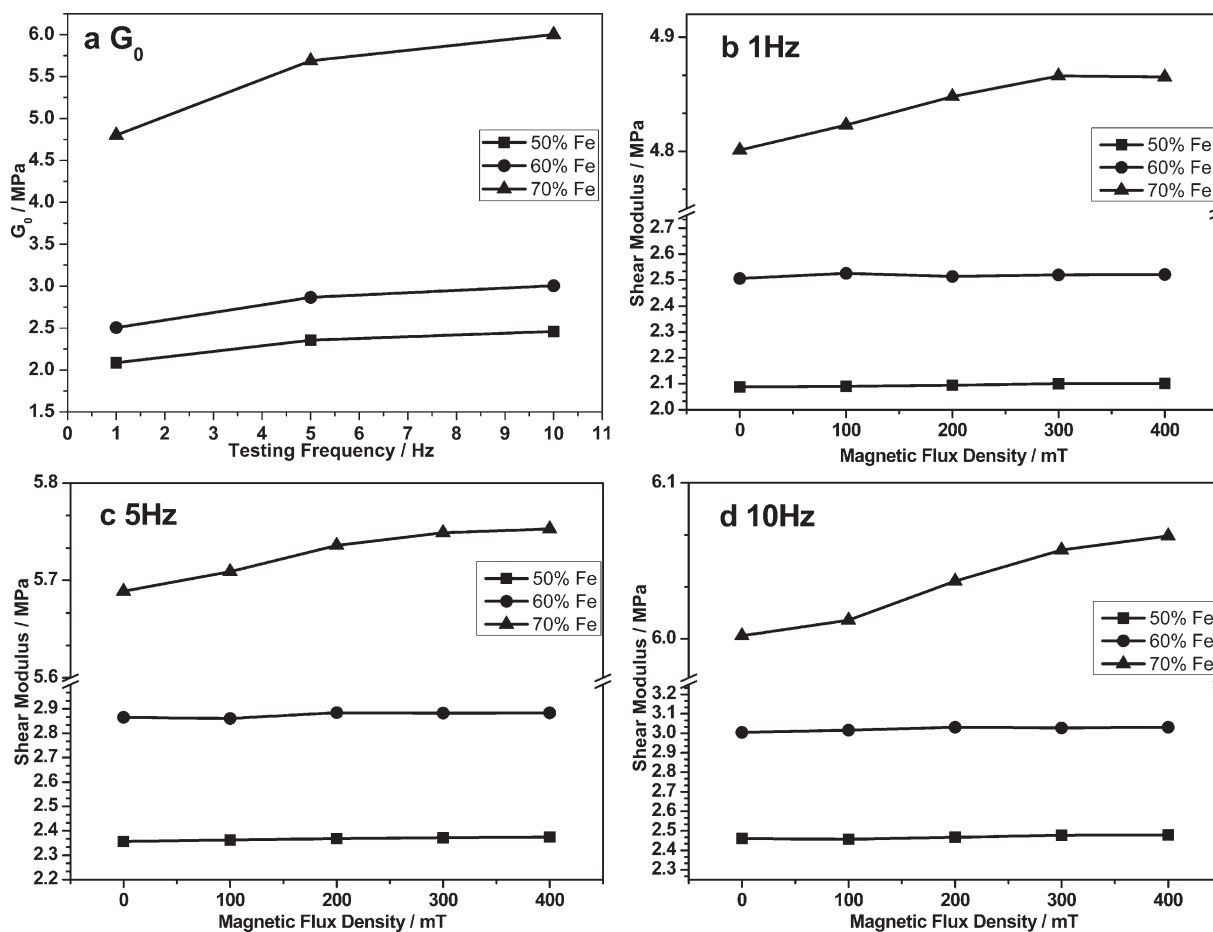


**Figure 10**  $G_0$  and magnetic field-induced shear modulus increment of PU MR elastomer prepared with treated carbonyl iron particles tested at different frequencies: (a)  $G_0$ , (b) 1 Hz, (c) 5 Hz, and (d) 10 Hz.

attributed to the stronger interaction between the carbonyl iron and PU matrix. From the viewpoint of practice use, both mechanical and magnetorheological properties are very important during the long-term service, a balance between two properties should be considered.

## References

- Rabinow, J. AIEE Trans 1948, 67, 1308.
- Carlson, J. D.; Weiss, K. D. U.S. Pat. 5,382,373 (1995).
- Shtarkman, E. M. U.S. Pat. 4,942,947 (1990).
- Watson, J. R. Mich. U.S. Pat. 5,609,353 (1997).
- Shiga, T.; Okada, A.; Kurauchi, T. J Appl Polym Sci 1995, 58, 787.
- Jolly, M. R.; Carlson, J. D.; Munoz, B. C.; Bullions, T. A. J Intell Mater Syst Struct 1996, 7, 613.
- Wilson, M. J.; Fuchs, A.; Gordaninejad, F. J Appl Polym Sci 2002, 84, 2733.
- Zhou, G. Y. Smart Mater Struct 2003, 12, 139.
- Kallio, M.; Lindroos, T.; Aalto, S.; Jarvinen, E.; Karna, T.; Meinander, T. Smart Mater Struct 2007, 16, 506.
- Ginder, J. M.; Nichols, M. E.; Elie, L. D.; Tardiff, J. L. Proc SPIE 1999, 3675, 131.
- Chen, L.; Gong, X. L.; Li, W. H. Polym Test 2008, 27, 340.
- Lokander, M.; Stenberg, B. Polym Test 2003, 22, 245.
- Lokander, M.; Stenberg, B. Polym Test 2003, 22, 677.
- Wang, Y. L.; Deng, H. X.; Gong, X. L.; Zhang, P. Q. Polym Eng Sci 2006, 46, 264.
- Shen, Y.; Golnaraghi, M. F.; Heppler, G. R. J Intell Mater Syst Struct 2004, 15, 27.
- Boczkowska, A.; Awietjan, S.; Babski, K.; Wroblewski, R.; Leonowicz, M. Proc SPIE 2006, 6170, 61700R-1.
- Boczkowska, A.; Awietjan, S.; Wroblewski, R. Smart Mater Struct 2007, 16, 1924.
- Fuchs, A.; Zhang, Q.; Elkins, J.; Gordaninejad, F.; Evrensel, C. J Appl Polym Sci 2007, 105, 2497.
- Furukawa, M.; Mitsui, Y.; Fukumaru, T.; Kojio, K. Polymer 2005, 46, 10817.
- Chen, L.; Gong, X. L.; Jiang, W. Q.; Yao, J. J.; Deng, H. X.; Li, W. H. J Mater Sci 2007, 42, 5483.
- Bailey, R.; Castle, J. E. J Mater Sci 1977, 12, 2049.
- Wang, Y. L.; Hu, Y.; Chen, L.; Gong, X. L.; Jiang, W. Q.; Zhang, P. Q.; Chen, Z. Y. Polym Test 2006, 25, 262.
- Sun, M. L. Application Principle and Theory of Epoxy Resins; China machine press: Beijing, 2002; p 18–24.
- Seymour, R. W.; Ester, G. M.; Cooper, S. L. Macromolecules 1970, 3, 579.
- Chen, T. K.; Tien, Y. I.; Wei, K. H. Polymer 2000, 41, 1345.
- Teo, L. S.; Chen, C. Y.; J Kuo., F. Macromolecules 1997, 30, 1793.
- Xia, H. S.; Song, M. Soft Matter 2005, 1, 386.
- Bajsic, E. G.; Rek, V. J Appl Polym Sci 2001, 79, 864.
- Lokander, M.; Reitberger, T.; Stenberg, B. Polym Degrad Stab 2004, 86, 467.